Supplementary Material

Tailoring Dielectric Performance via Dipole Density and Hydrogen-Bonding Interaction Towards High-Temperature Capacitive Energy Storage Polymer

Feng Zhou, Chong Tian, Lei Huang, Yunfeng Jiang, Fuqi Zhao, Na Yang, Dandan Yun, Xufu Cai

College of Polymer Science and Engineering, State Key Laboratory of Polymer Materials Engineering, Sichuan University, Chengdu 610065, China.

E-mail: caixf2008@scu.edu.cn

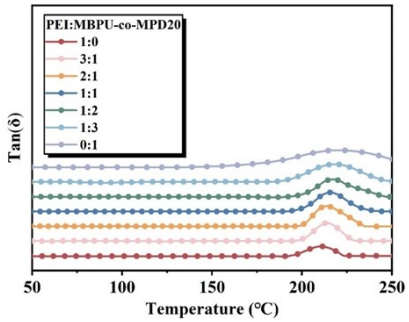

Fig S1. Tan(δ) curves of PEI/MBPU-co-MPD_{20} blends in DMA test.

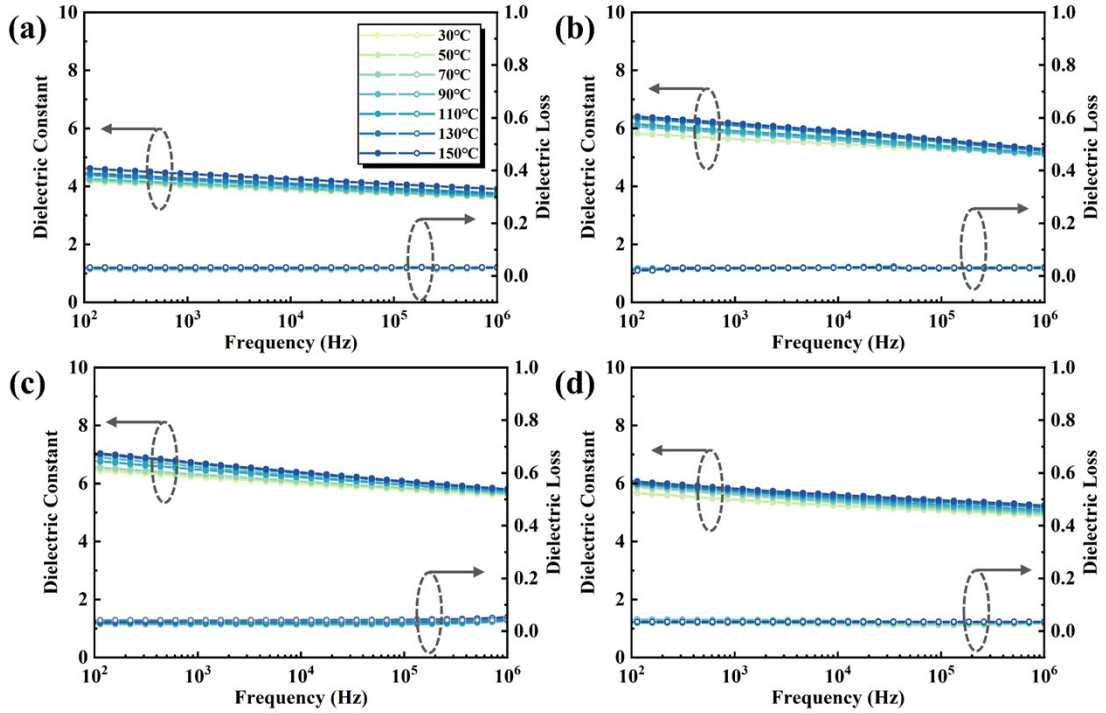

Fig S2. Dielectric constant and loss of PEI/MBPU-co-MPD_{20} blends at different mass ratios at 150 °C (a-3:1, b-2:1, c-1:2, d-1:3)

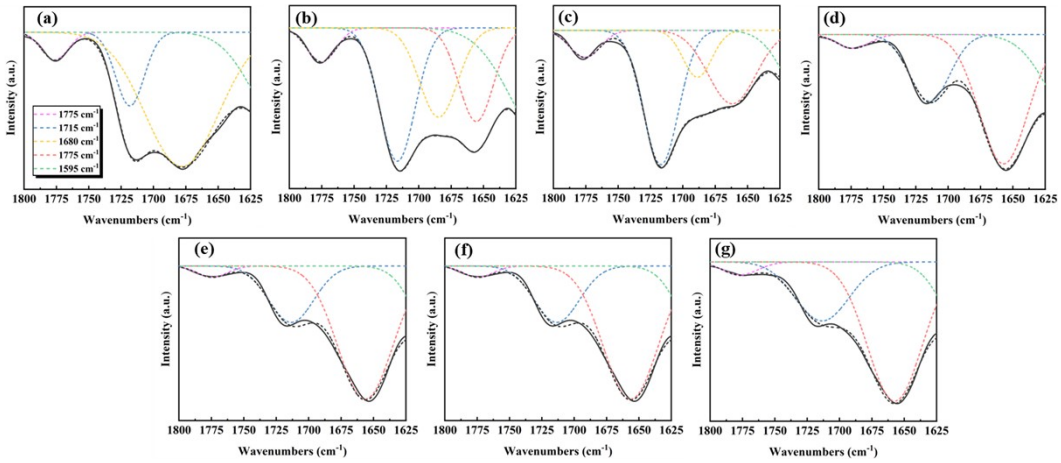

Fig S3. Comparison of FT-IR spectra and fractions of free C=O of PEI (a), MBPU-co-MPD_{20} (g) and PEI/co-polyurea blends with different PEI:MBPU-co-MPD_{20} ratios of 3:1 (b), 2:1 (c), 1:1 (d), 1:2 (e) and 1:3 (f).

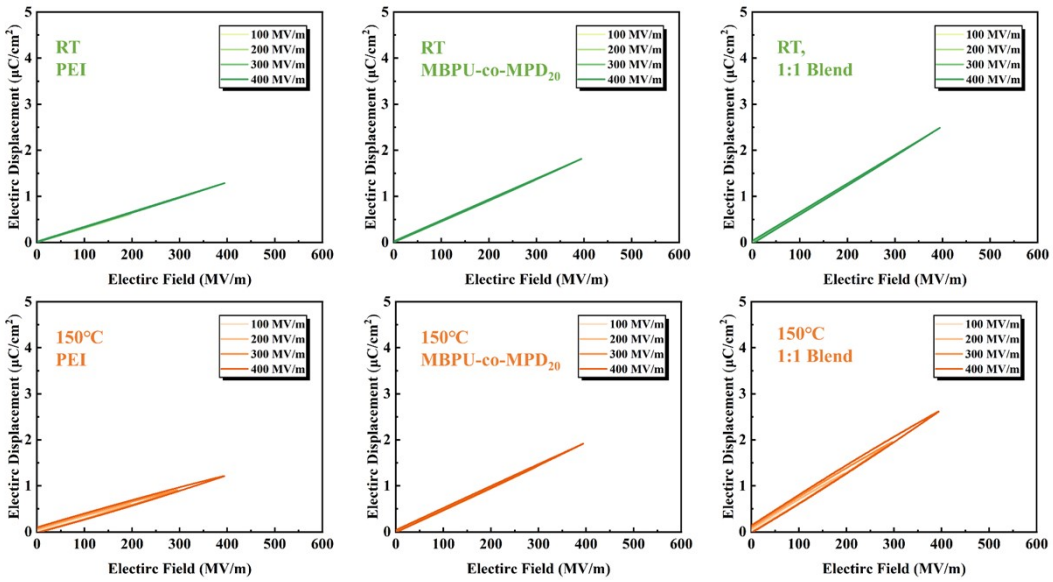

Fig S4. *D-E* loops of PEI, MBPU-co-MPD_{20} and the 1:1 blend dielectric films at room temperature and 150 °C.

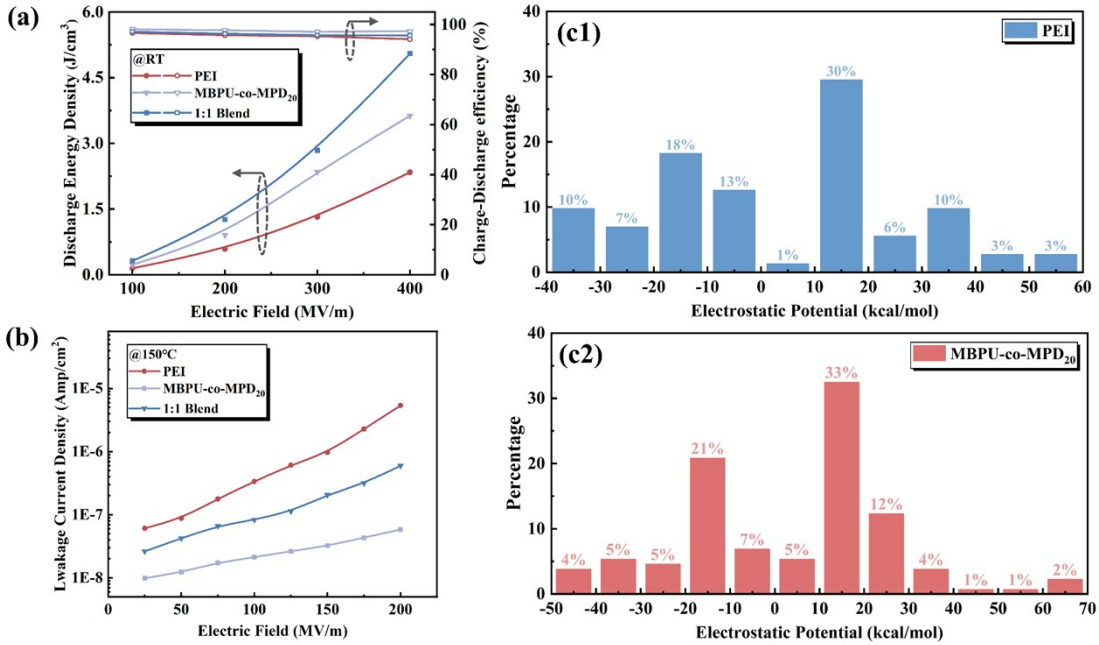

Fig S5. The charge-discharge efficiency of PEI, MBPU-co-MPD$_{20}$ and the 1:1 blend dielectric films (a) and leakage current density of PEI, MBPU-co-MPD$_{20}$ and the 1:1 blend dielectric films at 150°C. Surface electrostatic potential distribution (C).

Table S1. Molecular weights and distributions of the MBPU-co-MPD$_n$.

Sample	M_n	M_w	Polydispersity (PDI)
MBPU-co-MPD$_0$	47663	82314	1.7270
MBPU-co-MPD$_5$	37582	67264	1.7898
MBPU-co-MPD$_{10}$	38974	68532	1.7584
MBPU-co-MPD$_{20}$	33938	60781	1.7910
MBPU-co-MPD$_{30}$	5871	12238	2.0843
MBPU-co-MPD$_{40}$	4612	9736	2.1108
MBPU-co-MPD$_{50}$	3832	8293	2.1642

Table S2. Summary of glass Transition temperature (T_g) and dielectric property characterization for MBPU-co-MPD$_n$ at ambient temperature.

Sample	T_g (°C)	ε_r (1 kHz)	Tanδ (%, 1 kHz)	E_b (MV/m)
MBPU-co-MPD$_0$	215.2	4.19	1.36	685
MBPU-co-MPD$_5$	212.7	4.73	1.49	640
MBPU-co-MPD$_{10}$	213.1	4.99	1.44	592
MBPU-co-MPD$_{20}$	211.4	5.13	1.32	620
MBPU-co-MPD$_{30}$	200.1	3.60	2.62	287